# Polygons on the honeycomb lattice



1989 J. Phys. A: Math. Gen. 22 1371

(http://iopscience.iop.org/0305-4470/22/9/024)

J. Phys. A: Math. Gen. 22 (1989) 1371-1384. Printed in the UK

# Polygons on the honeycomb lattice

I G Enting† and A J Guttmann‡

CSIRO Division of Atmospheric Research, Private Bag 1, Mordialloc, Victoria 3195 Australia

‡ Department of Mathematics, University of Melbourne, Parkville, Victoria 3052, Australia

Received 17 August 1988

**Abstract.** We have enumerated the number of self-avoiding polygons on the honeycomb lattice to 82 steps. Analysis of the resulting series gives for the connective constant $\mu = 1.847\,7594 \pm 6 \times 10^{-6}$, in agreement with Nienhuis' value of $\mu = (2+\sqrt{2})^{1/2} = 1.847\,75906\ldots$. The critical exponent $\alpha = 0.4999 \pm 10^{-4}$ (unbiased), or $\alpha = 0.49998 \pm 2 \times 10^{-5}$ (biased). A non-physical singularity on the negative real axis is accurately located, and some curious results concerning the confluent singularity are obtained.

## 1. Introduction

This paper extends earlier work of Guttmann and Sykes (1973) in which the generating function for self-avoiding polygons on the honeycomb lattice was given to 34 terms. In the present paper we have extended this enumeration to 82 terms.

This considerable extension was made possible by improvements in several areas: firstly, in the algebraic techniques for enumerating polygons that span a finite rectangle, as detailed in the next section. Further improvements were achieved by rewriting our program to minimise page faulting and to more effectively utilise the memory allocation of the computer we used. Finally, improvements in computer technology enabled the resource demanding program to be run in a reasonable time.

We considered the honeycomb lattice polygon series particularly worthy of extension, as it is the only lattice on which the connective constant is exactly known, due to the work of Nienhuis (1982). His exact, but non-rigorous, result can be confirmed to high precision by analysis of our extended data, and the subsequent use of his exact result allows a highly accurate determination of the corresponding exponent $\alpha$.

Further, by analogy with various exactly solved models, we would expect the functional form of the polygon generating function to be simpler than that for other generating functions, such as that for the susceptibility. Thus our extended data might be useful in the search for an exact solution.

In the next section we describe the improvements to the generating function methods for enumerating honeycomb polygons, while § 3 describes the inclusion-exclusion relations which provide a way of combining the finite lattice data to give the infinite lattice results. We also give the exact generating function for the enumeration of convex polygons, the set of $n$-step polygons that can fit into a rectangle of perimeter $n$ steps, but no smaller rectangle. This enables us to extend our results by an additional two steps, as described in § 3, resulting in the 82-step series which is analysed in § 4. As well as the physical singularity, a non-physical singularity is found and its position located reasonably accurately.

0305-4470/89/091371+14$02.50  

## 2. Generating functions for enumerating polygons

The use of generating functions for enumerating polygons on two-dimensional lattices was described by Enting (1980) in his work on the enumeration of polygons on the square lattice. The relatively minor nature of modifications required to enumerate polygons on related lattices is shown in our work enumerating polygons on the L and Manhattan lattices (Enting and Guttmann (1985), which also reported an extension of the square lattice series). Our most recent work (Guttmann and Enting 1988a) further extends the square lattice series (to 56-step polygons) and includes the calculation of caliper moments. This most recent work also includes a number of results concerning the computational complexity of the calculations that carry over to the present analysis.

The algebraic generating function techniques have two requirements. The first is a technique for determining the number of polygons that span the length of a rectangle $W$ bonds wide by $L$ bonds long. The second requirement is a procedure for combining such enumerations to give the number of polygons per site on an infinite lattice. This latter problem is addressed in § 3 below.

The present calculations treat the honeycomb lattice as a sublattice of the square lattice. This can be done in terms of two distinct orientations as shown in figure 1. Since our algebraic techniques distinguish between the two square lattice axes, the orientations shown in figure 1 are significant. For reasons of efficiency we shall make use of both orientations. For each orientation the vertices are of two types, as shown in figure 1. The algebraic techniques enumerate polygons spanning the lengths of rectangles. We have to define two types of rectangles for each orientation and we do this according to the type of the first site (conventionally top left) that we insert when building up a rectangle.

The algebraic technique involves drawing a cross section line through the rectangle, intersecting a set of bonds and dividing the rectangle into two. The basic combinatorial

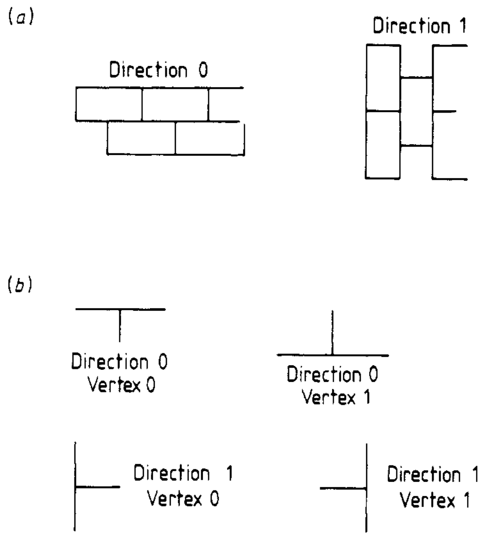


**Figure 1** (*a*) The two distinct orientations possible when representing the honeycomb lattice as a sublattice of the square lattice. (*b*) The two vertex types occurring in the respective orientations.

object is a state vector. Each component of such a vector is a generating function for loops in the region to the left of the cross section line $P$ that cut the cross section line in a specified pattern. The allowed patterns are described by Enting (1980). Each pattern can be represented by an ordered set of bond states $\langle n_1 \ldots n_m \rangle$, where

| | |
|---|---|
| $n_i = 0$ | empty bond |
| $= 1$ | link in part of loop being seen for the first time |
| $= 2$ | link in part of loop being seen for second time. |

These pattern arrays are subject to the constraint that the sequence $n_1$ to $n_k$ must never, for any $k$, contain more 2s than 1s and the numbers of 1s and 2s in the total sequence must be equal. (As a technical point, we regard the 0, 1, 2 specification of the pattern as digits in a base-4 integer and use this integer as an index for the state vector, using a hash-addressing scheme. The use of base 4 allows us to use bit masking to recover bond states.) A generating function expression for the number of allowed patterns of a given length (and thus for the size of the state vector) is given by Guttmann and Enting (1988a, equation (10)). Enting (1980 figures 1, 2 and 3; equations (2.2)-(2.4)) gives a detailed description of the way in which movement of the cross section line corresponds to transformation of the algebraic expression.

We enumerate polygons in finite rectangles by moving the cross section line through the rectangle, adding one site at a time. Initially the cross section line will cut the two bonds leading into the next site to be added. After adding the site, these two bonds will no longer cut the cross section line but two new bonds will. The addition of a site thus corresponds transforming states 'in' into states 'out' in all allowable ways. In its simplest form, changing from a square lattice to a restricted lattice (e.g. L, Manhattan or honeycomb) simply corresponds to a restriction on the number of ways that are allowed. Such restrictions will depend on the orientation and vertex type.

Figure 2 lists the possible inputs in the leftmost column. The second column lists the possible outputs for the full square lattice (based on figure 8 of Enting 1980). The next four columns give the allowed outputs for the honeycomb lattice, classified according to orientation and vertex type. As entry of 'na' indicates that the input is not allowed to occur in that context, in the sense that any such occurrence (for which we test) would indicate a program failure and not simply a zero-weight configuration. As in all our previous polygon enumerations we introduce 'ghost' bonds extending beyond the rectangle so that, so far as is possible, boundary sites are treated equivalently to internal sites. The main exceptions occur at the lowest site. In this case, outputs with a non-zero state in the vertical bond (i.e. the ghost bond) are not permitted. Inputs with a 2 in the lowest horizontal bond (corresponding to $n_1 = 2$) are an error condition for which we test.

Treating the honeycomb lattice as a restricted square lattice with the output states specified in columns 2–6 of figure 2 is quite a powerful technique for enumerating polygons on the honeycomb lattice. In the course of the present study we used the technique to extend the polygon enumeration to 46 steps.

However, this direct approach makes inefficient use of space when enumerating polygons using orientation 1. In this case about half the square lattice bonds cut by the cross section line must be in state 0 because of the restrictions on the lattice. The precise positions of these bonds will depend on the position of the kink in the cross section line and the vertex type of the top of the column, i.e. many different subsets of the full set of square lattice pattern arrays are required as the construction proceeds.

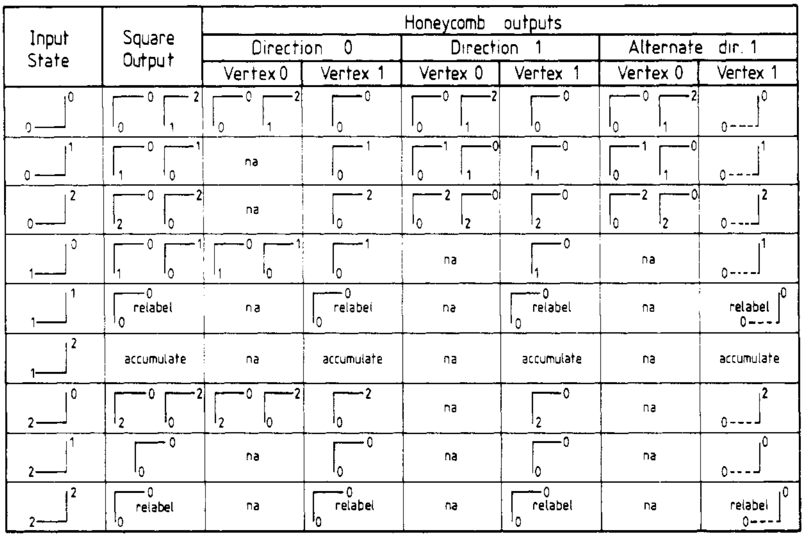


**Figure 2.** Bond-state transition matrix for adding one site. The left-most column lists all allowed input states. The second column lists corresponding allowed output states for the unrestricted square case. Columns 3–6 list output states for the honeycomb lattice, classified according to orientation and vertex type. Entries marked na denote forbidden inputs, for a particular case. Columns 7 and 8 are the allowed outputs for vertex types 0 and 1 using the alternative representation for orientation 1.

We are able to achieve a much more efficient use of space by letting our patterns involve mainly actual bonds of the honeycomb lattice. We introduce a single 'ghost' bond to preserve the formal '2-in', '2-out' nature of our site-addition rules. Our procedure for doing this is shown in figure 3. When a type-0 site is added a real bond and a ghost bond are replaced by the two real bonds. When a type-1 vertex is added, two real bonds are replaced by a real bond and a ghost bond. In this approach, the

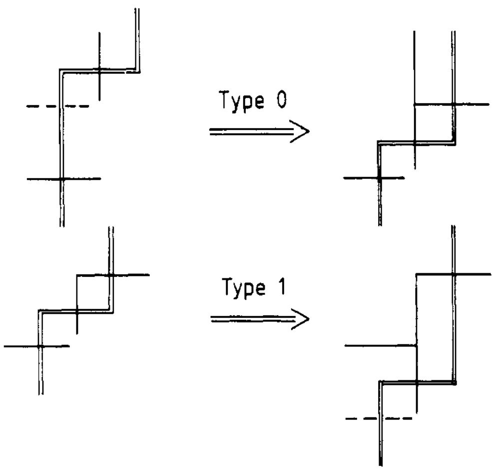


**Figure 3.** The use of an internal ghost bond (dotted) in the modified approach to orientation 1.

set of allowable patterns is a dense subset of the full set of allowable square lattice patterns. One point to note is that after adding a type-1 vertex, the two output bonds become the two input bonds for the next site addition. After adding a type-0 vertex only one of the output bonds is used in the new input. The new inputs are obtained by shifting one place to the left in the array of pattern indices. In all our previous enumerations (square, L, Manhattan and direct approach to the honeycomb) we used techniques that moved one place along the pattern array every time a site was added.

The requirement of stepping along the pattern array, only after adding type-0 vertices in the present case is to be expected since the size of the pattern array will be of order half the width. The last columns of figure 2 show the allowed outputs for the various inputs when using this approach. Figures 4 and 5 show the process of adding a full column to rectangles of width 3 and 4. These diagrams illustrate two important details. The first is that if the last site was of type 1 then the pattern index has to be reset by shifting one place before working on the next column. This procedure, shifting the ghost bond from bottom to top, was used in all previous enumerations. However, if a type-0 site occurs at the bottom of a column then the pattern index has to be shifted two places. The second point to note is that if the width is odd then the number of elements required in the pattern array alternates from column to column. This must be taken into account when setting the starting position in the pattern array.

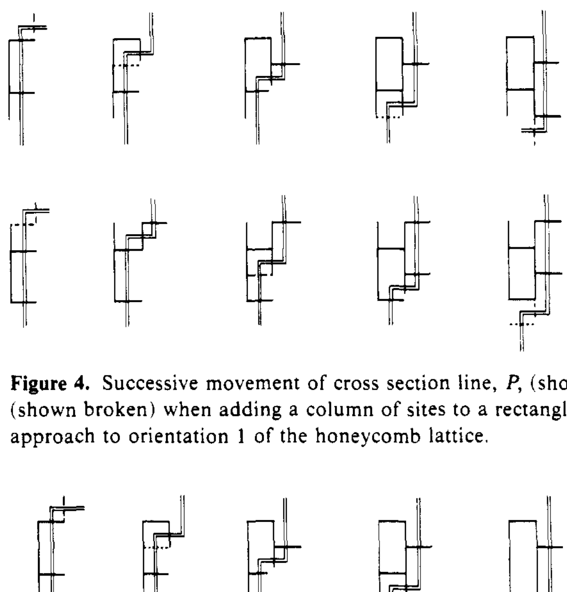

**Figure 4.** Successive movement of cross section line, $P$, (shown double) and ghost bonds (shown broken) when adding a column of sites to a rectangle of width 3 for the modified approach to orientation 1 of the honeycomb lattice.

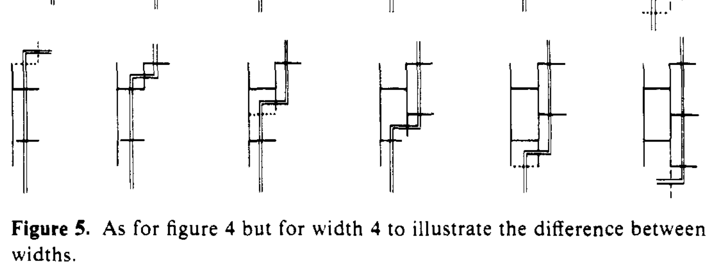

**Figure 5.** As for figure 4 but for width 4 to illustrate the difference between odd and even widths.

For an even width, $W$, $B=2+W/2$ bonds are required. For an odd width, the number alternates between $2+(W+1)/2$ and $2+(W-1)/2$. Thus an odd width will (for half the columns) require as many bonds as the succeeding even width. For the lattices considered in our earlier work and for the 0 orientation of the honeycomb lattice the number of bonds is $W+2$. Thus for a given number of bonds, and consequently a given limit on the size of the state vector, the rectangles that can be treated in the 1 orientation are twice as wide as can be treated in the 0 orientation. (It should be noted that we specify widths of rectangles in terms of numbers of bonds rather than numbers of sites. This agrees with our recent publications but Enting (1980) expressed widths in terms of numbers of sites.) We use a maximum of $B=15$ which requires a state vector with 113 634 components (Guttmann and Enting 1988a).

## 3. Inclusion–exclusion relations

The inclusion-exclusion relations provide a way of combining polygon enumerations on finite rectangles to give the infinite lattice limit. Such inclusion-exclusion relations for rectangles (defined in terms of the inverse of an incidence matrix) were exploited in the computational techniques used by de Neef and Enting (1977). Their use has been simplified by the explicit relations obtained by Enting (1978). The reduced symmetry of the honeycomb lattice requires the consideration of four distinct cases where only one case was involved for the square lattice. The symmetry involved and the consequences for inclusion-exclusion relations, are precisely the same on the honeycomb lattice as for the checkerboard Potts model considered by Enting (1987). In previous polygon enumeration, the Manhattan lattice involved consideration of two cases (two types of site) while the L lattice involved only one case because translation from one class of site into the other was simply equivalent to reversal of all the directed bonds.

For the honeycomb lattice, we consider the lattice fixed in the '1' orientation for the purposes of distinguishing width and length as the vertical and horizontal dimensions in our diagrams.

Let $g^i_{mn}$ be the generating function for polygons that fit into a rectangle of width $m$ and length $n$ with the top left vertex of type $i=0, 1$ but not into any smaller rectangle.

We put

$$g_{mn}=g^0_{mn}+g^1_{mn}. \tag{1}$$

For the infinite lattice, the polygon generating function is

$$C(x)=\sum_{mn} g_{mn} \tag{2a}$$

$$=\sum_{\substack{m,n\\ m+n\leqslant k}} g_{mn} \qquad \text{correct to } x^{2k}. \tag{2b}$$

The quantities computed by the procedures of the previous section are, from working in the '1' orientation

$$H^i_{mn}=g^i_{mn}+g^i_{m-1,n}+g^{1-i}_{m-1,n}+2g^i_{m-2,n}+g^{1-i}_{m-2,n}\ldots \tag{3}$$

or, more simply,

$$H_{mn}=H^0_{mn}+H^1_{mn}=\sum_{j=1}^{m}(m-j+1)g_{jn} \tag{4}$$

and from working in the '0' orientation,

$$G^i_{mn} = g^i_{mn} + g^i_{m,n-1} + g^{1-i}_{n,m-1} + 2g^i_{m,n-2} + g^{1-i}_{m,n-2} \dots$$

or

$$G_{mn} = \sum_{j=1}^{n} (n-j+1) g_{nj}. \tag{5}$$

Relations (4) and (5) are inverted as

$$g_{mn} = H_{mn} - 2H_{m-1,n} + H_{m-2,n} \tag{6a}$$

$$g_{mn} = G_{mn} - 2G_{m,n-1} + G_{m,n-2} \tag{6b}$$

and the relations

$$\sum_{m=1}^{k} g_{mn} = H_{kn} - H_{k-1,n} \tag{7a}$$

and

$$\sum_{n=1}^{k} g_{mn} = G_{mk} - G_{m,k-1} \tag{7b}$$

can be readily derived from (6$a$, $b$) or directly from (4) and (5).

In evaluating the sum (2$b$), we will use $H_{mn}$ for $m = 1$ to $2W$ and $G_{mn}$ for $n = 1$ to $W$ i.e. $H_{mm}$ is evaluated using the 1 orientation with $m$ as the width and $G_{mn}$ is evaluated in the 0 orientation with $n$ as the width.

This enables us to evaluate (2$b$) as

$$C(x) \simeq \sum_{\substack{m,n \\ m+n \leqslant 3W+1}} g_{mn} \qquad \text{correct to } x^{6W+2}. \tag{8}$$

For small $m, n$ we have a choice as to whether we evaluate $g_{mn}$ in terms of $H_{mn}$ or $G_{mn}$. The development is simplest if we retain the arbitrary nature of the division. We simply require two limit functions $p(\cdot)$ and $q(\cdot)$ such that

$$C(x) \simeq \sum_{\substack{m,n \\ m+n \leqslant 3W+1}} g_{mn} = \sum_n \sum_{m=1}^{p(n)} g_{mn} + \sum_m \sum_{n=1}^{q(m)} g_{mn} \tag{9a}$$

$$= \sum_n (H_{p(n),n} - H_{p(n)-1,n}) + \sum_m (G_{m,q(m)} - G_{m,q(m)-1}). \tag{9b}$$

As in all generating function expressions, generating functions with zero or negative indices are set to zero. We use

$$p(n) = 3W + 1 - n \qquad n \geqslant W+1 \tag{10a}$$

$$= W + n \qquad n \leqslant W \tag{10b}$$

and

$$q(m) = 3W + 1 - m \qquad m \geqslant 2W+1 \tag{11a}$$

$$= m - W - 1 \qquad m \leqslant 2W. \tag{11b}$$

There is an additional modification that can be made to improve the efficiency of the calculation. We can express the polygon generating function as

$$C(x) \simeq \sum_{mn} g_{mn} = \sum_{mn} \{a_{mn}(H^0_{mn} + H^1_{mn}) + b_{mn}(G^0_{mn} + G^1_{mn})\} \tag{12}$$

with all the coefficients $a_{mn}$, $b_{mn}$ either $-1$, 0 or 1 by virtue of (9*b*). For odd $j$ we have, from the obvious geometrical symmetry,

$$H^0_{jn} = H^1_{jn} \qquad \text{and} \qquad G^0_{mj} = G^1_{mj}.$$

Thus for odd $j$ we can replace $a_{jn}(H^0_{jn} + H^1_{jn})$ by $2a_{jn}H^0_{jn}$ and $b_{mj}(G^0_{mj} + G^1_{mj})$ by $2b_{mj}(G^0_{mj})$. These transformations remove the requirement for half of the transfer matrix calculations for odd widths. This achieved a 20% reduction in computer time for odd $W$.

The other symmetry relations do not give a similar reduction. Most rectangles of odd length must still be processed as a step towards treating longer even-length rectangles. An additional improvement could be achieved by modifying the limit of the summation for type-0 rectangles of even width because in the sum (9*a*) the longest rectangles of even width will have odd length. However the potential improvement is too small for it to be worth introducing yet another special case.

As in the square lattice case (Guttmann and Enting 1988a) the inclusion-exclusion relations provide a basis for calculating the correction terms required to extend the series. The summation in (9*a*) with $W = 13$ enumerates all polygons that can fit into rectangles with perimeter $p \leqslant 80$. This gives all polygons with $n \leqslant 80$ and all 82-step polygons with $p \leqslant 80$. This represents all 82-step polygons except for those for which $p = n = 82$. The set of polygons with $n$ steps that can fit into a rectangle of perimeter $n$ but not into any smaller rectangles, were referred to as convex polygons by Guttmann and Enting (1988b). The convexity property is defined in terms of the square lattice and this definition has no natural interpretation on the honeycomb lattice. For example, figure 6 shows that honeycomb lattice polygons may, when mapped onto the square

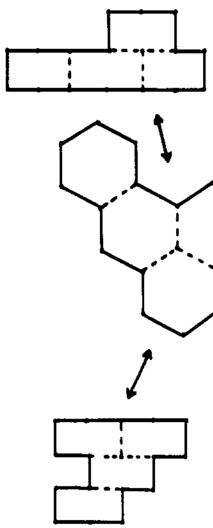

**Figure 6.** Mapping of a honeycomb lattice onto a sublattice of the square lattice showing how the square lattice convexity property can depend on the orientation of the mapping. Thus our convexity property has no natural interpretation on the honeycomb lattice.

lattice, be either convex or non-convex depending on their orientation. Thus, unlike the square lattice, the convex honeycomb lattice polygons are of little interest except as correction terms in the present analysis.

These convex polygons can be readily enumerated as on the square lattice. Guttmann and Enting (1988b) noted that for orientation 1, recurrence relations for the honeycomb lattice were given by restricting the ranges of the summations that occurred in the square lattice case. Two types of rectangle must be considered and the results are not rotationally invariant. These differences involve trivial changes to the square lattice enumeration procedure and so the enumeration can be easily extended to the limits of the available machine integer size or further if residue arithmetic is

**Table 1.** Coefficients of the polygon generating function, where $c_{2n}$ is the number of $2n$-step polygons embeddable on the honeycomb lattice.

| $n$ | $c_n$ |
|---|---|
| 6 | 1 |
| 8 | 0 |
| 10 | 3 |
| 12 | 2 |
| 14 | 12 |
| 16 | 18 |
| 18 | 65 |
| 20 | 138 |
| 22 | 432 |
| 24 | 1 074 |
| 26 | 3 231 |
| 28 | 8 718 |
| 30 | 25 999 |
| 32 | 73 650 |
| 34 | 220 215 |
| 36 | 643 546 |
| 38 | 1 937 877 |
| 40 | 5 783 700 |
| 42 | 17 564 727 |
| 44 | 53 222 094 |
| 46 | 163 009 086 |
| 48 | 499 634 508 |
| 50 | 1 542 392 088 |
| 52 | 4 770 925 446 |
| 54 | 14 832 934 031 |
| 56 | 46 227 584 010 |
| 58 | 144 632 622 552 |
| 60 | 453 628 244 950 |
| 62 | 1427 228 330 481 |
| 64 | 4 500 947 210 772 |
| 66 | 14 231 512 500 103 |
| 68 | 45 095 972 401 236 |
| 70 | 143 219 294 049 399 |
| 72 | 455 745 199 043 542 |
| 74 | 1 453 111 646 955 645 |
| 76 | 4 641 449 091 849 300 |
| 78 | 14 851 454 597 198 009 |
| 80 | 47 598 148 798 881 660 |
| 82 | 152 789 607 567 089 925 |

used. However as with the square lattice, a relatively small number of terms suffice for determining a recurrence relation

$$\begin{aligned}[(n+1)^2-12(n+1)+20]p_{2n+2}-[4n-22]p_{2n}-[7(n-1)^2-60(n-1)+52]p_{2n-2}\\ -[2(n-2)^2-24(n-2)+20]p_{2n-4}+[12(n-3)^2-52(n-3)-16]p_{2n-6}\\ +[8(n-4)^2-24(n-4)-32]p_{2n-8}\\ =20\delta_{n,-1}+22\delta_{n,0}-52\delta_{n,1}+8\delta_{n,2}+4\delta_{n,3}+8\delta_{n,4}\end{aligned}$$

where the coefficients $p_{2m}$ are the number of $(2m+6)$-step convex polygons embeddable on the honeycomb lattice, with generating function $P(x)=\Sigma_{n=0}^{\infty} p_{2n}x^n$, and $p_{2m}=0$ for $m<0$. This corresponds to the differential equation for the generating function

$$\begin{aligned}P''(x)(x^2-7x^4-2x^5+12x^6+8x^7)+P'(x)(-11x-4x^2+53x^3+22x^4-40x^5-16x^6)\\ +P(x)(20+22x-52x^2-20x^3-16x^4-32x^5)\\ =20+22x-52x^2+8x^3+4x^4+8x^5\end{aligned} \tag{13}$$

which has the solution

$$P(x)=[1-2x+x^2-x^4-x^2(1-4x^2)^{1/2}]/[(1+x)(1-2x)]^2. \tag{14}$$

The singularity structure on the real axis is the same as for convex polygons on the square lattice, that is, a confluent exponent of $\frac{1}{2}$, and a leading exponent of 2 at the critical point $x=\frac{1}{2}$. In addition, there is a singularity at $x=-1$ which has no counterpart on the square lattice. The required correction term is $p_{82}=703, 245, 931, 702$.

These conjectured results have subsequently been confirmed by Lin and Chang (1988). We have recently learned that the results for the square lattice were in fact first obtained by Delest and Viennot (1984).

The series to 82 terms is given in table 1. It required two runs on a Cyber 990, each taking 18 hours of CPU time, and 20 hours of monitor time (reflecting massive page faulting). A third run confirmed our results. Each sum uses the arithmetic of integers modulo a given prime, which allows integers larger than those which can be stored for use (Guttmann and Enting 1988a). We used the two largest primes less than $2^{15}$. In this way the least significant digits are given, while the method of differential approximants was used to obtain the most significant digits. This approach is described in greater detail in Guttmann and Enting (1988a).

## 4. Analysis of series

We have analysed the polygon-generating function by the method of differential approximants, utilising the scheme developed in Guttmann (1987), which was also used for the analysis of the square lattice generating function in Guttmann and Enting (1988a). The results of the *unbiased* analysis are given in the first four columns of table 2. We combine these entries using the method described in Guttman (1987), which is simple statistical procedure that involves a weighted mean of those table entries that have an error less than some multiple of the smallest error of the individual errors given. In this case the multiple was precisely 5, so that only those entries orresponding to $n=33$, 35, 36, 37 and 38 were used in the final estimate of the critical exponent based on first-order differential approximants. The errors referred to above are in all

**Table 2.** Summary of exponent and critical point estimates using (*a*) first- and (*b*) second-order differential approximants. Biased exponent estimates are also given. The column labelled $N$ implies that coefficients to order $x^{2N+6}$ were used in the analysis and the column labelled $l$ gives the number of approximants used in forming the averages quoted at each order. If $l<4$, the entry is not used in the overall error analysis.

(*a*)

| $N$ | Critical point | Error | Exponent | Error | $l$ | Biased exponents | Error | $l$ |
|---|---|---|---|---|---|---|---|---|
| 22 | 0.292 8964 | — | 1.504 30 | — | 1 | 1.503 238 | (8233) | 10 |
| 23 | — | — | — | — | 0 | 1.499 868 | (4436) | 10 |
| 24 | 0.292 8951 | (30) | 1.499 31 | (80) | 2 | 1.499 192 | (1783) | 10 |
| 25 | — | — | — | — | 0 | 1.500 081 | (1830) | 11 |
| 26 | 0.292 8989 | (70) | 1.498 03 | (238) | 3 | 1.500 191 | (2169) | 12 |
| 27 | 0.292 8926 | (130) | 1.500 14 | (416) | 5 | 1.499 552 | (3002) | 11 |
| 28 | 0.292 8934 | (107) | 1.500 16 | (399) | 8 | 1.500 204 | (500) | 12 |
| 29 | 0.292 8918 | (93) | 1.500 61 | (389) | 9 | 1.500 134 | (290) | 12 |
| 30 | 0.292 8930 | (36) | 1.500 19 | (161) | 12 | 1.500 054 | (261) | 12 |
| 31 | 0.292 8929 | (67) | 1.500 18 | (295) | 11 | 1.499 965 | (467) | 10 |
| 32 | 0.292 8925 | (33 | 1.500 38 | (159) | 10 | 1.500 009 | (113) | 11 |
| 33 | 0.292 8934 | (12) | 1.499 97 | (57) | 9 | 1.500 028 | (99) | 10 |
| 34 | 0.292 8929 | (17) | 1.500 16 | (83) | 11 | 1.500 062 | (63) | 11 |
| 35 | 0.292 8928 | (10) | 1.500 27 | (55) | 11 | 1.500 028 | (35) | 9 |
| 36 | 0.292 8932 | (10) | 1.500 03 | (53) | 11 | 1.500 051 | (110) | 12 |
| 37 | 0.292 8931 | (4) | 1.500 09 | (24) | 11 | 1.500 029 | (25) | 11 |
| 38 | 0.292 8930 | (2) | 1.500 14 | (14) | 12 | 1.500 022 | (12) | 9 |

(*b*)

| $N$ | Critical point | Error | Exponent | Error | $l$ | Biased exponents | Error | $l$ |
|---|---|---|---|---|---|---|---|---|
| 24 | — | — | — | — | — | 1.500 132 | — | 1 |
| 25 | 0.292 8998 | — | 1.498 16 | — | 1 | 1.500 473 | — | 1 |
| 26 | 0.292 8941 | — | 1.500 15 | — | 1 | 1.500 378 | (267) | 2 |
| 27 | — | — | — | — | 0 | 1.501 402 | — | 1 |
| 28 | 0.292 8854 | (11) | 1.502 67 | (181) | 2 | 1.500 446 | (749) | 3 |
| 29 | 0.292 8893 | (63) | 1.501 78 | (292) | 3 | 1.500 116 | (300) | 4 |
| 30 | 0.292 8922 | (31) | 1.500 45 | (121) | 4 | 1.500 023 | (80) | 4 |
| 31 | 0.292 8921 | (34) | 1.500 39 | (129) | 6 | 1.499 944 | (102) | 7 |
| 32 | 0.292 8951 | (73) | 1.498 70 | (490) | 7 | 1.499 938 | (95) | 5 |
| 33 | 0.292 8948 | (33) | 1.498 85 | (295) | 7 | 1.500 030 | (243) | 7 |
| 34 | 0.292 8947 | (32) | 1.498 89 | (210) | 8 | 1.499 985 | (45) | 8 |
| 35 | 0.292 8901 | (70) | 1.500 50 | (110) | 6 | 1.499 996 | (38) | 7 |
| 36 | 0.292 8922 | (33) | 1.500 37 | (147) | 5 | 1.500 028 | (51) | 7 |
| 37 | 0.292 8933 | (20) | 1.499 91 | (94) | 7 | 1.500 030 | (21) | 8 |
| 38 | 0.292 8932 | (8) | 1.500 07 | (39) | 8 | 1.500 040 | (31) | 7 |

cases two standard deviations about the mean, and these are shown parenthesised in table 2.

Combining the tabulated results gives

$$x_c^2 = 0.292\,8930\,(2) \qquad 2-\alpha = 1.500\,11\,(13) \qquad \text{(first order)}$$

$$x_c^2 = 0.292\,8932\,(8) \qquad 2-\alpha = 1.500\,22\,(36) \qquad \text{(second order).}$$

These results do not display quite the level of precision seen in the analysis of the square lattice series, which had errors about a factor of 3 smaller than those given for first-order approximants, and about a factor of 10 smaller for second-order approximants. Nevertheless, they are still highly accurate and provide strong support for both the result of Nienhuis (1982) that $x_c^2 = 1 - 1/\sqrt{2} = 0.292\,893\,2188\ldots$, and for the result that $2-\alpha = \frac{3}{2}$ which follows from Nienhuis's result that $\nu = \frac{3}{4}$ together with hyperscaling.

Unlike the square lattice, one knows the exact critical point in this case, so *biased* approximants can also be constructed. These give estimates of $2-\alpha$, and are also summarised in table 2, in the fifth and sixth columns. Combining these results as above gives

$$2-\alpha = 1.500\,025\,(12) \qquad \text{(first order)}$$

$$2-\alpha = 1.500\,020\,(15) \qquad \text{(second order)}$$

estimates which are an order of magnitude more accurate than the unbiased estimates. We attach no real significance to the fact that the error bounds are so tight as to just exclude the believed exact result. As discussed in Guttmann and Enting (1988a) this is believed to be due to the fact that our procedure does not attempt to extrapolate any trends in the data, as we believe that this should be a distinct operation. However, in this case there is no obvious trend to extrapolate.

The slight inferiority of this data compared with the square lattice data can, we believe, be ascribed to the presence of an additional (non-physical) singularity on the negative real $x_c^2$ axis in the honeycomb case. This singularity maps to a conjugate pair of singularities on the imaginary axis in the complex $x$ plane, and is responsible for the well known four-term periodicity of the ratio plots seen in the honeycomb self-avoiding walk generating function (Guttmann 1987). This situation is also present in the corresponding Ising model series, except in that case the honeycomb lattice has a conjugate pair of singularities on the imaginary axis at $\pm i v_c$, whereas for the walks generating function we find the imaginary singularities to be outside the circle of convergence. We have carried out an analysis similar to that described above for the non-physical singularity, and find the following estimates:

$$x_c^2 = -0.412\,38\,(15)\ \text{exponent} = 1.44\,(3) \qquad \text{(first order)}$$

$$x_c^2 = -0.412\,22\,(54)\ \text{exponent} = 1.46\,(8) \qquad \text{(second order).}$$

It is quite plausible that this exponent is exactly 1.5, particularly as the corresponding non-physical exponent in the honeycomb Ising model free energy is equal to the corresponding exponent at the critical point, both being 2. Tentatively accepting this value, a re-analysis of the data biased at an exponent of 1.5 yields an estimate for the position of the non-physical singularity of $x_c^2 = -0.412\,06\,(5)$ or, equivalently $x_c^{-2} = -2.4268\,(3)$. It is interesting to note that $-2-(2+\sqrt{2})/8 = -2.426\,776\ldots$, while it is known that the physical singularity satisfies $x_c^{-2} = 3.414\,21\ldots = 2+\sqrt{2}$. While this agreement is quite likely fortuitous, it nevertheless provides a useful mnemonic, lying as it does in the centre of the estimated numerical range. In the event that it is correct, it may provide useful insight into the structure of the exact solution of the polygon generating function.

Another aspect of our analysis worthy of comment is our attempt to find evidence of a confluent singularity. In our previous analysis of the square lattice data, we commented that we found no evidence of a non-analytic correction-to-scaling exponent, and pointed out that this was in agreement with the correction-to-scaling exponent predicted by Neinhuis (1982, 1984) $\Delta = 1.5$, as the value of the physical critical exponent

($\frac{3}{2}$) meant that the confluent term was indistinguishable from the analytic background term. (This remark does not apply to the self-avoiding walk generating function, where the physical critical exponent is $\frac{43}{32}$.) For the honeycomb polygon series the critical point is exactly known, so that the method of Baker and Hunter (1973) for analysing confluent singularities can be used. As the method requires a divergent series if there is any analytic background term, the series has been differentiated four times, so that it should now diverge with an exponent of $2+\alpha=2.5$. The results are shown in the left-hand side of table 3, where the pole(s) give the reciprocal of the exponent(s), and the residues give estimates of an amplitude which is not of interest in the present application. There is evidence of only one exponent, and the data may be summarised as $1/\gamma_1=0.3998\pm0.0003$, or $\gamma_1=2.501\pm0.002$. As expected, there is no evidence of a confluent singularity.

Almost as an afterthought, we repeated this analysis for the square lattice data. The results are also shown in table 3, and it is clear that as well as the expected singularity at $1/\gamma_1=0.400\pm0.006$, there is a second singularity on the positive real axis at $1/\gamma_2=0.503\pm0.030$, or $\gamma_2=2.00\pm0.01$. Such a singularity in the fourth derivative of the polygon generating function integrates to a singularity of the form $(1-z/z_c)^2\ln|1-z/z_c|$ in the generating function, or a correction to scaling exponent $\Delta=\frac{1}{2}$. We find this result quite surprising. There is no evidence for it from other methods of analysis we have tried, yet it appears quite strongly on the basis of this analysis, though it is noteworthy that it only becomes apparent with polygons longer than 38

**Table 3.** Poles of Padé approximants to four-times-differentiated square and honeycomb polygon generating function series, transformed by Baker–Hunter transformation to identify confluent singularities.

| Honeycomb lattice | | | | Square lattice | | | |
|---|---|---|---|---|---|---|---|
| $N$ | $[N-1/N]$ | $[N/N]$ | $[N+1/N]$ | $N$ | $[N-1/N]$ | $[N/N]$ | $[N+1/N]$ |
| 7 | | | | 7 | 0.377 86 | 0.391 70 | 0.395 95 |
| 8 | | | | 8 | 0.399 63 | 0.398 94 | 0.395 79* |
| | | | | | 0.555 70 | 0.595 19 | — |
| 9 | 0.398 18 | 0.398 22 | 0.398 58 | 9 | 0.399 62 | — | 0.399 12 |
| | — | — | — | | 0.555 94 | — | — |
| 10 | 0.398 18* | 0.398 70 | 0.398 58 | 10 | 0.402 47 | 0.403 40 | 0.402 77 |
| | — | — | — | | 0.500 37 | 0.487 91 | 0.497 71 |
| 11 | 0.398 00 | 0.399 05 | 0.398 44 | 11 | 0.402 99 | 0.403 42* | 0.400 76 |
| | — | — | — | | 0.493 60 | 0.487 81 | 0.557 23 |
| 12 | 0.396 97 | 0.39948 | 0.397 71 | 12 | 0.402 57 | 0.398 44 | |
| | — | — | — | | 0.499 14 | — | |
| 13 | — | 0.399 77 | 0.401 38 | | | | |
| | — | — | 0.491 83 | | | | |
| 14 | 0.400 67 | 0.399 84 | 0.399 98 | | | | |
| | 0.588 84 | — | — | | | | |
| 15 | 0.399 97 | 0.399 85 | 0.399 86 | | | | |
| | — | — | — | | | | |
| 16 | 0.399 86 | 0.399 85 | 0.399 81 | | | | |
| | — | — | — | | | | |
| 17 | 0.399 81 | 0.399 86 | 0.399 81 | | | | |
| | — | — | — | | | | |
| 18 | 0.399 81 | 0.399 83 | | | | | |

steps. Further, there is no evidence of such a singularity from the honeycomb data, and universality considerations lead us to expect the same confluent exponent in both cases, though this could perhaps be explained by a very small amplitude in the honeycomb case. Indeed, it may be that the attributes of the honeycomb lattice that allow the critical point to be obtained are exactly such as to cause the amplitude of the confluent term to vanish. Saleur (1987) investigated the corrections to scaling by studying the transfer matrix spectrum. In this way he obtained two such exponents, $\Delta_1 = \frac{1}{2}$ and $\Delta_2 = \frac{11}{16}$. However, the first exponent $\Delta_1$ corresponds to a particular operator which is a total derivative, and hence cannot contribute to corrections to scaling. Thus conformal invariance theory predicts a possible correction-to-scaling exponent $\Delta = \frac{11}{16}$. This value is slightly higher than that which we have found. We conclude with this vexing question left open.

## Acknowledgments

We would like to thank Darryl Chivers for assistance in running our program on the University of Melbourne Cyber 990. Financial support from the Australian Research Grants to one of us (AJG) is acknowledged.

## References

Baker G A Jr and Hunter D L 1973 *Phys. Rev.* B **7** 3377
Delest M-P and Viennot G 1984 *Theor. Comput. Sci.* **34** 169-206
de Neef T and Enting I G 1977 *J. Phys. A: Math. Gen.* **10** 801-5
Enting I G 1978 *J. Phys. A: Math. Gen.* **11** 563-8
—— 1980 *J. Phys. A: Math. Gen.* **13** 3713-22
—— 1987 *J. Phys. A: Math. Gen.* **20** 1917-21
Enting I G and Guttmann A J 1985 *J. Phys. A: Math. Gen.* **18** 1007-17
Guttmann A J 1987 *J. Phys. A: Math. Gen.* **20** 1839
Guttmann A J and Enting I G 1988a *J. Phys. A: Math. Gen.* **21** L165-72
—— 1988b *J. Phys. A: Math. Gen.* **21** L467-74
Guttmann A J and Sykes M F 1973 *Aust. J. Phys.* **26** 207
Lin K Y and Chang S J 1988 *J. Phys. A: Math. Gen.* **21** 2635-42
Nienhuis B 1982 *Phys. Rev. Lett.* **49** 1062
—— 1984 *J. Stat. Phys.* **34** 731
Saleur H 1987 *J. Phys. A: Math. Gen.* **20** 455